Phys Chem Minerals (2017) 44:323–334
DOI 10.1007/s00269-016-0860-3

ORIGINAL PAPER

Ferrorhodonite, $CaMn_3Fe[Si_5O_{15}]$, a new mineral species from Broken Hill, New South Wales, Australia

Nadezhda V. Shchipalkina[1,2] · Nikita V. Chukanov[3] · Igor V. Pekov[1] · Sergey M. Aksenov[2,4,5] · Catherine McCammon[6] · Dmitry I. Belakovskiy[7] · Sergey N. Britvin[5] · Natalya N. Koshlyakova[1] · Christof Schäfer[8] · Ricardo Scholz[9] · Ramiza K. Rastsvetaeva[2]

Received: 31 August 2016 / Accepted: 4 November 2016 / Published online: 17 November 2016

Abstract The new mineral ferrorhodonite, a Mn^{2+}–Fe^{2+} ordered analogue of rhodonite with the idealized formula $CaMn_3Fe[Si_5O_{15}]$, was found in the manganese-rich metamorphic rocks of the Broken Hill Pb–Zn–Ag deposit, Yancowinna Co., New South Wales, Australia. Ferrorhodonite occurs as brownish red coarsely crystalline aggregates in association with galena, chalcopyrite, spessartine, and quartz. The mineral is brittle. Its Mohs hardness is 6. Cleavage is perfect on {201} and good on {021} and {210}. The measured and calculated values of density are 3.71 (2) and 3.701 g cm^{-3}, respectively. Ferrorhodonite is optically biaxial positive, with $\alpha = 1.731$ (4), $\beta = 1.736$ (4), $\gamma = 1.745$ (5) and 2 V (meas.) = 80 (10)°. The average chemical composition of ferrorhodonite is (electron-microprobe data, wt%): CaO 7.09, MgO 0.24, MnO 32.32, FeO 14.46, ZnO 0.36, SiO_2 46.48, and total 100.95. The empirical formula calculated on 15 O *apfu* ($Z = 2$) is $Ca_{0.81}Mn_{2.92}Fe_{1.29}Mg_{0.04}Zn_{0.03}Si_{4.96}O_{15}$. The Mössbauer and IR spectra are reported. The strongest reflections in the powder X-ray diffraction pattern [(d, Å (I, %) (hkl)] are: 3.337 (32) (−1–13), 3.132 (54) (−210), 3.091 (41) (0–23), 2.968 (100) (−2–11), 2.770 (91) (022), 2.223 (34) (−204), 2.173 (30) (−310). Ferrorhodonite is isostructural with rhodonite. The crystal structure was solved based on single-crystal X-ray diffraction data and refined to $R_1 = 4.02\%$ [for 3114 reflections with $I > 2\sigma(I)$]. The mineral is triclinic, space group $P\bar{1}$, $a = 6.6766$ (5), $b = 7.6754$ (6), $c = 11.803$ (1) Å, $\alpha = 105.501$ (1)°, $\beta = 92.275$ (1)°, $\gamma = 93.919$ (1)°; $V = 580.44$ (1). The crystal-chemical formula of ferrorhodonite inferred to be: $^{M5}(Ca_{0.81}Mn_{0.19})$ $^{M1-3}(Mn_{2.52}Fe_{0.48})$ $^{M4}(Fe^{2+}_{0.81}Mn_{0.12}Mg_{0.04}Zn_{0.03})$ $[Si_5O_{15}]$. .

Keywords Ferrorhodonite · Rhodonite · New mineral species · Pyroxenoid · Crystal structure · Mössbauer spectroscopy · Cation order · Broken Hill · Australia

✉ Nadezhda V. Shchipalkina
Estel58@yandex.ru

1 Faculty of Geology, Moscow State University, Vorobievy Gory, Moscow, Russia 119991

2 Institute of Crystallography, Russian Academy of Sciences, Leninsky Prospekt 59, Moscow, Russia 117333

3 Institute of Problems of Chemical Physics, Russian Academy of Sciences, Chernogolovka, Moscow Region, Russia 142432

4 Nesmeyanov Institute of Organoelement Compounds, Russian Academy of Sciences, GSP-1, Vavilova St. 28, V-334, Moscow, Russia 119991

5 Department of Crystallography, St Petersburg State University, University Embankment 7/9, St. Petersburg, Russia 199034

6 Bayerisches Geoinstitute, University of Bayreuth, Universitätsstraße 30, 95440 Bayreuth, Germany

7 Fersman Mineralogical Museum of the Russian Academy of Sciences, Leninsky Prospekt 18-2, Moscow, Russia 119071

8 Südwestdeutsche Salzwerke AG, Salzgrundstraße 67, 74076 Heilbronn, Germany

9 Departamento de Geologia, Escola de Minas, Universidade Federal de Ouro Preto (UFOP), Campus Morro do Cruzeiro, Ouro Prêto, MG 35400-000, Brazil

Introduction

Rhodonite is a rather widespread and well-known pyroxenoid. This mineral crystallizes over a wide range of temperatures and pressures and is an important component of manganese-rich skarns, metamorphic rocks, and postmagmatic hydrothermal associations. As a result, rhodonite samples from different deposits are characterized by a

rather wide chemical and crystal-chemical variability. The idealized formula for rhodonite is usually written as $CaMn_4Si_5O_{15}$ ($Z = 2$) (Minerals 1981; Back 2014). However, an analysis of the literature data and our investigation of more than one hundred samples of rhodonite from different localities (mainly from the collections of the Fersman Mineralogical Museum of the Russian Academy of Sciences, Moscow, Russia) by electron microprobe show wide variations of contents of both major and minor metal cations (Ca, Mn, Fe, Mg, Zn), in *apfu*: from 0.34 to 1.86 for Ca, from 2.85 to 4.66 for Mn, from 0 to 1.28 for Fe, from 0 to 0.68 for Mg, and from 0 to 0.56 for Zn. These variations result in the occurrence of rhodonite-type minerals with different schemes of cation order over the five *M* sites in the crystal structure.

In this paper, we report the results of thorough studies of a rhodonite-type mineral from Broken Hill, Yancowinna Co., New South Wales, Australia, which differs from all earlier known rhodonite samples by the highest content of FeO: 14.5 wt%. It was approved by the IMA CNMNC as a new mineral species, ferrorhodonite (Cyrillic: феррородонит), with the idealized formula $CaMn_3Fe[Si_5O_{15}]$, IMA No. 2016-016. It was named as an analogue of rhodonite with Fe^{2+} prevailing at the *M*4 site of the structure. The sample was received by Christof Schäfer in 1993 from a mining worker during his visit to the Broken Hill deposit.

Parts of the holotype specimen of ferrorhodonite are deposited in the collection of type specimens (Typmineralsammlung) of the Mineralogical Museum of the University of Hamburg, with the catalogue number MMHH-004704, and in the collection of the Fersman Mineralogical Museum, with the registration number 4847/1.

Occurrence

Broken Hill is a well-known, huge sedimentary exhalative lead, zinc and silver deposit which had been altered by metamorphism of the granulite facies (T ~ 850 °C, p ~ 5–7 kbar) with progressive melting in the range of 600–700 °C, which resulted in the enrichment the polymetallic melts in Cu and Pb. The intense deformation of orebody occurred during 5–15 million years after the peak of metamorphism (Frost et al. 2005; Walters 1998). More than 380 minerals were found here. Among them, Mn-rich pyroxenoids belonging to bustamite, rhodonite, and pyroxmangite structure types play an important role as principal manganese-bearing silicates in the primary ores. This mineralization was formed in T ~ 700–800 °C when the melts were saturated by Fe, Zn, Mn, and Si (Frost et al. 2002). Rhodonite in Broken Hill occurs mostly in the primary ores, in the pyroxenoid rock, which consists of bustamite, Mn-rich clinopyroxene, rare wollastonite, calcite, pyroxmangite, and Mn-rich olivine (Frost et al. 2005). This rock, in particular, is the major source of striking rhodonite crystals. Some finds of rhodonite samples belong to the zone of massive kaolinite and presumably represent retrograted mineral assemblages. Primary rhodonite ranges from microscopic inclusions in sulfides to large aggregates. Typical associated minerals are galena, spessartine, sphalerite, calcite, hedenbergite, bustamite, fluorite, and quartz (Birch 1999).

Based on the data by Frost et al. (2002, 2005), we consider that ferrorhodonite was crystallized during the progressive melting in the temperature range 700–800 °C. The process of saturation the polymetallic melt by Fe, Mn, and Si caused the presence of ferrorhodonite in the polymetallic ores.

Physical properties

General appearance, associated minerals, and mechanical properties

Ferrorhodonite forms aggregates composed by thick tabular to short prismatic crystals, with rounded edges, up to 2 cm across (Fig. 1). Associated minerals are galena, chalcopyrite, spessartine, and quartz.

The new mineral is brown-red to pinkish brown. Some pieces are transparent in thin sections. The streak is white. Ferrorhodonite does not demonstrate fluorescence in ultraviolet radiation. The mineral is brittle, with stepped fracture. Its Mohs hardness is 6. Cleavage is perfect on {201} and good on {021} and {210} (according to optical data and by analogy with rhodonite). The density measured by hydrostatic weighing is close to the density calculated based on the empirical formula: their values are 3.71 (2) and 3.701 g cm^{-3}, respectively.

Fig. 1 Aggregate of ferrorhodonite (*red crystals*) in galena

Optical properties

Ferrorhodonite is optically biaxial positive, with $\alpha = 1.731$ (4), $\beta = 1.736$ (4), $\gamma = 1.745$ (5) (589 nm), 2 V (meas.) = 80 (10)° and 2 V (calc.) = 74°. Dispersion of optical axes is distinct, $r < v$. Under the microscope, the mineral is colorless and non-pleochroic.

Infrared spectroscopy

In order to obtain an infrared (IR) absorption spectra, powdered samples have been mixed with dried KBr, pelletized, and analyzed using an ALPHA FTIR spectrometer (Bruker Optics) with a resolution of 4 cm^{-1} and 16 scans (Fig. 2). The IR spectrum of an analogous pellet of pure KBr was used as a reference.

The IR spectrum of ferrorhodonite is very close to that of Fe-poor rhodonite (Chukanov 2014). This fact is expected because masses and force characteristics of the cations Fe^{2+} and Mn^{2+} are close. Bands of OH groups (in the range 3000–4000 cm^{-1}) are absent in the IR spectrum of ferrorhodonite.

Mössbauer spectroscopy

The Mössbauer spectrum was recorded at room temperature (293 K) in transmission mode on a constant-acceleration Mössbauer spectrometer with a nominal 370 MBq ^{57}Co high specific activity source in a Rh matrix 12 μm thick. The velocity scale was calibrated relative to α-Fe foil 25 μm thick using the positions certified for former National Bureau of Standards standard reference material no. 1541; line widths of 0.36 mm s^{-1} for the outer lines of α-Fe were obtained at room temperature. The measurement of the spectrum took four days, and it was fit using the program MossA (Prescher et al. 2012).

The spectrum was fit to two Lorentzian quadrupole doublets with component widths and areas constrained to be equal (Fig. 3): the doublet with quadrupole splitting QS = 2.42 mm s^{-1}, isomer shift IS = 1.19 mm s^{-1} and relative area $S = 62.5 \pm 2\%$ and the doublet with QS = 1.29 mm s^{-1}, IS = 1.06 mm s^{-1} and $S = 37.5 \pm 2\%$.

Chemical data

The electron-microprobe data for ferrorhodonite were obtained using a JEOL JXA-8230 instrument (EDS mode) at the Laboratory of Analytical Techniques of High Spatial Resolution, Department of Petrology, Moscow State University. Standard operating conditions included an accelerating voltage of 20 kV and a beam current of 10 nA. Standards for quantitative analysis were: wollastonite for Ca, diopside for Mg, Mn for Mn, orthopyroxene for Fe and Si, and Zn for Zn. The results of analyses are presented in Table 1. The analyses 1–4 present the variation of chemical composition for ferrorhodonite.

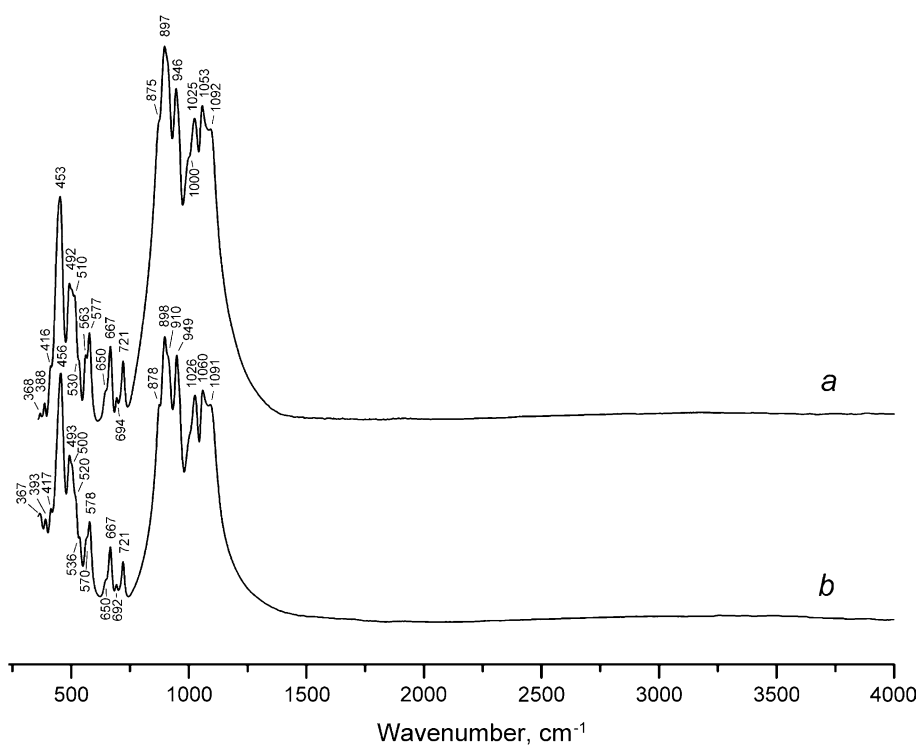

Fig. 2 Infrared absorption spectra of *a* ferrorhodonite and *b* rhodonite with composition $Ca_{0.9}Mn_{3.7}Mg_{0.4}(Si_5O_{15})$ from Långban, Sweden

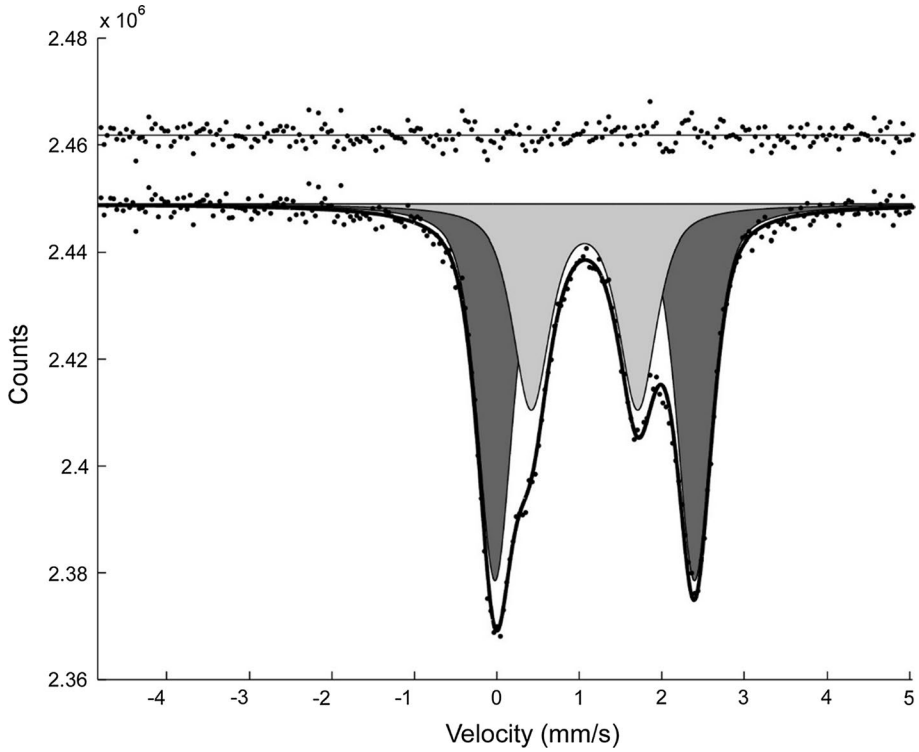

Fig. 3 Mössbauer spectrum of ferrorhodonite. Two doublets corresponding to Fe^{2+} are *shaded dark* and *light gray*

Table 1 Chemical composition of ferrorhodonite (1–4) and Fe-rich rhodonite (wt%): 5–7—Broken Hill, New South Wales, Australia; 8—Simsio, Finland; 9—Prilukskoe, Ukraine; 10—Yuzhnoe, Dalnegorsk area, Primorskiy Kray, Russia

Component wt%	1	2	3	4	Mean for 1–4	5	6	7	8	9	10
SiO_2	46.45	46.58	46.41	46.48	46.48	46.45	46.15	46.2	46.28	47.11	48.29
Al_2O_3							0.93				
FeO	14.47	14.50	14.47	14.39	14.46	12.77	10.51	9.03	11.11	9.42	7.20
MnO	32.16	32.45	32.35	32.33	32.32	35.10	38.62	39.72	39.72	42.19	42.95
MgO	0.24	0.25	0.21	0.25	0.24	0.40	1.41	0.12	0.14	1.78	0.19
ZnO	0.36	0.36	0.38	0.35	0.36			0.30			
CaO	7.09	7.11	7.11	7.04	7.09	5.45	2.01	4.66	2.87	1.72	4.75
Total	100.77	101.25	100.93	100.84	100.95	100.17	99.63	100.03	100.12	102.26	103.42
Formula calculated based on 15 O *apfu*											
Si	4.96	4.96	4.96	4.96	4.96	4.99	4.96	4.99	5.00	4.97	5.02
Al							0.12				
Fe	1.29	1.29	1.29	1.28	1.29	1.15	0.94	0.82	1.00	0.83	0.63
Mn	2.91	2.93	2.93	2.92	2.92	3.19	3.51	3.63	3.64	3.77	3.78
Mg	0.04	0.04	0.03	0.04	0.04	0.06	0.23	0.02	0.02	0.28	0.03
Zn	0.03	0.03	0.03	0.03	0.03			0.02			
Ca	0.80	0.80	0.80	0.79	0.80	0.62	0.23	0.53	0.33	0.19	0.52
Number of cations	5.07	5.09	5.08	5.06	5.08	5.02	4.99	5.02	4.99	5.07	4.96

5–6 Henderson and Glass (1936); 7–Mason (1973); 8–Hietanen (1938); 1–4, 9, 10–our data

The empirical formula calculated for mean chemical data on the basis of 15 O *apfu* is $(Ca_{0.80}Mn_{2.92}Fe_{1.29}Mg_{0.04}Zn_{0.03})_{\Sigma 5.09}$ $Si_{4.96}O_{15}$. The simplified formula is $CaMn_3FeSi_5O_{15}$.

The Gladstone–Dale compatibility index is: $1 - (K_p/K_c) = 0.011$ ("superior").

X-ray diffraction data

Powder X-ray diffraction data (Table 2) were collected using a Rigaku R-AXIS Rapid II diffractometer (image plate), Co*Kα* (λ = 1.78897 Å), 40 kV, 15 mA, rotating anode with the microfocus optics, Debye–Scherrer geometry, $d = 128.4$ mm, exposure 15 min. Calculated intensities were obtained by means of STOE WinXPOW v. 2.08 program suite based on the atomic coordinates and unit-cell parameters obtained from the single-crystal data. The data (in Å for Co*Kα* radiation) are listed in Table 2. The parameters of triclinic unit cell refined from the powder data are: $a = 6.683$ (2), $b = 7.674$ (2), $c = 11.806$ (2) Å, $\alpha = 105.50$ (3)°, $\beta = 92.26$ (2)°, $\gamma = 93.93$ (2)°, $V = 581.0$ (3) Å^3.

The single-crystal X-ray diffraction experiment was realized using a Bruker SMART APEX2 diffractometer (Bruker 2009) with graphite-monochromatized MoK_α radiation (λ = 0.71073 Å). The raw data were integrated by using the program SAINT and then scaled, merged, and corrected for Lorentz-polarization effects using the SADABS package. The total of 7879 reflections within the sphere limited by $\theta = 30.80°$ were obtained. The experimental details of data collection and refinement values are shown in Table 3. The parameters triclinic unit cell are: $a = 6.6766$ (5), $b = 7.6754$ (6), $c = 11.803$ (1) Å, α = 105.501 (1)°, $\beta = 92.275$ (1)°, $\gamma = 93.919$ (1)°; space group $P\bar{1}$. After averaging the equivalent reflections, the experimental set contained 3114 reflections with $I > 2\sigma(I)$. As initial model for structural refinement, we used the coordinates of rhodonite (Peacor and Niizeki 1963). The structure refinement was realized by using the JANA2006 package of programs (Petříček et al. 2006). Atomic scattering factors for neutral atoms together with anomalous dispersion corrections were taken from *International Tables for X-Ray Crystallography* (Ibers and Hamilton 1974). Graphic visualization of the structure was produced using a combination the JANA2006 program package and the Diamond software (Brandenburg and Putz 2005). The final cycle of refinement cycles gave $R_1 = 4.02\%$, $wR_2 = 6.30\%$, GOF = 0.99 for all data. Fractional atomic coordinates, equivalent atomic displacement parameters (U_{eq}), and anisotropic atomic displacement parameters U_{ij} are given in Tables 4 and 5, respectively. The occupancies of *M*1–*M*4 sites by Fe and Mn were fixed during the refinement because Mn and Fe have close number of electrons and cannot be distinguished by means of X-ray diffraction. Selected interatomic distances are presented in Table 6.

Discussion

Chemical composition

Finds of iron-rich rhodonite are rare in nature. Such samples are known mostly from the Broken Hill deposit (Table 1). Some rhodonite samples with high Fe content (analyses 9–10) from the collection of the Fersman Mineralogical Museum originated in metamorphic Mn-rich metasedimentary rocks of the Prilukskoe manganese deposit (Chivchines, Ukraine) and skarns of the Yuzhnoe base-metal deposit (near Dalnegorsk, Primorskiy Kray, Russia). Average FeO content in a large number of rhodonite samples, described in previous publications (Henderson and Glass 1936; Hietanen 1938; Leverett et al. 2008; Mason 1973; Nelson and Griffen 2005) and determined by us, is approximately ~2.5 wt% (with variations from 0.0 to 5.0 wt%). This mean corresponds to 0.22 *apfu* of Fe in empirical formula (with variations from 0.0 to 0.5 *apfu*, respectively) In Fe-rich samples the content of FeO exceeds the average mean by 3–5 times (Table 1) and the formula coefficient for Fe in such samples varies from 0.5 to 1.0 *apfu*. However, the distribution of Fe among *M*(1–5) sites in the crystal structure can vary (Table 7) and needs special studies using other methods besides X-ray diffraction.

The crystal structure of rhodonite-type minerals

The crystal structure of rhodonite was solved by Liebau et al. (1959) and Peacor and Niizeki (1963), and later redetermined and refined (Peacor et al. 1978; Ohashi and Finger 1975; Nelson and Griffen 2005). It contains chains of tetrahedra with a repeat unit $[Si_5O_{15}]$ and ribbons formed by edge-sharing polyhedra *M*1, *M*2, *M*3, *M*4, and *M*5 (Fig. 4). The polyhedra *M*1, *M*2, and *M*3 are weakly distorted octahedra with mean cation-oxygen distances in the range 2.21–2.23 Å, predominantly occupied by Mn^{2+}. The polyhedron *M*4 is a strongly distorted octahedron with the shortest and the longest cation-oxygen distances lying in the ranges 1.95–1.98 and 2.77–2.91 Å, respectively. This site concentrates Fe^{2+}, Mg, and Zn (Peacor and Niizeki 1963; Ohashi and Finger 1975; Peacor et al. 1978; Nelson and Griffen 2005). The shortest *M*4–O distances are observed in rhodonite samples with highest contents of small cations, Mg^{2+} and Fe^{2+} (Peacor et al. 1978; Dickson 1975). The site *M*5 has sevenfold coordination, mean cation-oxygen distances in the range 2.40–2.42 Å, and in most cases, is predominantly occupied by Ca (usually, together with subordinate Mn).

Table 2 Powder X-ray diffraction data for ferrorhodonite

I_{meas}	d_{meas}	I_{calc}	d_{calc}	h	k	l	I_{meas}	d_{meas}	I_{calc}	d_{calc}	h	k	l
3	11.38	4	11.35	0	0	1	24	2.595	25	2.593	2	−2	1
		1	7.371	0	1	0	8	2.548	3	2.548	0	−3	1
13	7.131	9	7.127	0	−1	1			1	2.529	−2	−1	3
22	6.654	16	6.649	1	0	0	25	2.518	23	2.517	0	−3	2
28	4.765	21	4.764	−1	−1	1	6	2.478	5	2.477	1	2	2
3	4.191	1	4.194	1	0	2	14	2.456	12	2.455	2	1	2
15	4.122	8	4.118	1	−1	2	7	2.431	2	2.432	−2	−2	1
		1	4.076	1	1	1			6	2.426	2	0	3
13	3.820	4	3.823	0	−2	1	4	2.397	2	2.400	1	−3	2
		3	3.812	0	−1	3	7	2.378	2	2.382	−2	−2	2
4	3.686	3	3.686	0	2	0			3	2.375	0	−3	3
22	3.565	13	3.563	0	−2	2			1	2.374	2	2	0
11	3.414	9	3.411	1	−2	1	5	2.345	4	2.345	−2	1	3
		11	3.342	−1	2	0	7	2.323	4	2.325	−1	−3	1
32	**3.337**	4	3.334	−1	−1	3	7	2.277	4	2.277	0	3	1
		11	3.324	2	0	0			2	2.229	−2	2	2
		2	3.281	1	−1	3			2	2.228	2	2	1
		4	3.256	0	2	1	**34**	**2.223**	16	2.226	−2	0	4
13	3.248	8	3.244	−2	0	1			21	2.220	0	−2	5
5	3.208	2	3.207	1	0	3	9	2.198	2	2.200	−3	0	1
		7	3.140	2	0	1	**30**	**2.173**	30	2.172	−3	1	0
54	**3.132**	37	3.128	−2	1	0	11	2.153	5	2.151	3	0	1
41	**3.091**	12	3.092	0	−2	3			2	2.125	−3	1	1
		12	3.088	−1	−2	2	19	2.111	16	2.112	−1	−2	5
		2	3.048	0	1	3			1	2.108	−3	0	2
		21	2.972	−2	1	1	20	2.101	19	2.099	1	3	1
100	**2.968**	55	2.966	−2	−1	1	9	2.066	5	2.064	2	−3	2
		3	2.947	−2	0	2			1	2.061	0	3	2
89	**2.929**	80	2.928	0	−1	4	6	2.048	1	2.054	−2	−2	4
		2	2.862	−1	1	3			1	2.044	−2	1	4
		2	2.826	1	2	1	6	2.003	2	2.001	−2	2	3
		5	2.803	−2	−1	2	7	1.974	5	1.974	3	−2	1
		2	2.796	2	0	2	6	1.953	2	1.952	0	−3	5
		6	2.783	−1	−2	3	5	1.932	2	1.930	−2	0	5
91	**2.770**	100	2.768	0	2	2			2	1.903	2	3	0
		2	2.742	2	1	1			1	1.902	0	−4	1
7	2.688	3	2.688	1	1	3			4	1.896	−2	−3	3
9	2.677	3	2.675	−2	1	2			1	1.895	2	1	4
27	2.652	24	2.651	1	−1	4			2	1.894	1	1	5
		1	2.617	0	−2	4	12	1.895	4	1.891	2	−1	5
									1	1.872	1	2	4

I_{meas}	d_{meas}	I_{calc}	d_{calc}	h	k	l	I_{meas}	d_{meas}
10	1.870	4	1.871	3	1	2	10	1.545
		3	1.868	0	−4	3	7	1.514
10	1.866	2	1.866	−3	−2	1	15	1.475
		3	1.864	3	0	3	7	1.464
5	1.857	3	1.855	−2	−2	5	6	1.455
		2	1.843	0	4	0	7	1.441

Table 2 continued

I_{meas}	d_{meas}	I_{calc}	d_{calc}	h	k	l	I_{meas}	d_{meas}
4	1.842	1	1.841	−1	−2	6	24	1.431
4	1.838	2	1.839	2	2	3	9	1.416
		1	1.834	3	2	0	7	1.399
		5	1.827	−2	3	2	8	1.383
4	1.824	2	1.823	1	−2	6	6	1.380
3	1.819	1	1.818	3	−2	3	6	1.370
		3	1.815	−1	4	0	4	1.362
5	1.808	6	1.806	2	3	1	3	1.347
		1	1.800	−3	0	4	5	1.342
4	1.774	3	1.774	−1	−4	3	5	1.338
5	1.745	3	1.745	0	−3	6	6	1.334
		1	1.742	3	−1	4	7	1.331
3	1.740	1	1.740	1	4	0	6	1.328
		5	1.726	−1	4	1	4	1.303
17	1.725	22	1.724	0	1	6	4	1.301
5	1.708	2	1.707	2	−4	1		
		8	1.694	3	−2	4		
17	1.693	12	1.693	2	−3	5		
15	1.688	8	1.687	−1	−3	6		
10	1.680	7	1.679	−2	3	3		
14	1.660	15	1.659	−4	0	1		
9	1.645	6	1.645	−3	−1	5		
11	1.641	9	1.639	1	1	6		
4	1.634	2	1.634	4	−1	1		
5	1.624	5	1.622	0	0	7		
5	1.615	1	1.615	−1	4	2		
13	1.604	11	1.604	−2	4	1		
		2	1.603	2	0	6		
11	1.599	3	1.598	−1	0	7		
		1	1.593	−2	−4	3		
11	1.587	4	1.588	−3	−3	3		
		8	1.582	−3	3	2		
2	1.562	2	1.562	4	−2	1		
10	1.558	4	1.558	2	4	0		
		3	1.557	−4	0	3		

Peaks with d below 2.20 Å could not be indiced unambiguously because of multiple overlapping reflections

The most intensive reflections are shown in bold

Different schemes of cation site occupancies in structurally investigated rhodonite samples are shown in Table 7. In most cases, the sites *M*1, *M*2, *M*3, and *M*4 are Mn-dominant, and the site *M*5 is Ca-dominant. In some samples Mn predominates in all five *M* sites (Ohashi and Finger 1975; Nelson and Griffen 2005). In rhodonite sample studied by Nelson and Griffen (2005), Mn and minor Fe occupy *M*1 and *M*2; at *M*4 Mg and Zn occur along with Mn and Fe; Mn and subordinate Ca occupy the *M*3 and *M*5 sites. In the rhodonite sample described by Ohashi and Finger (1975) Mn and Mg occupy *M*1, *M*2, and *M*3 sites; some amount of Fe is located at *M*4 site; Ca and Mn occupy *M*5 site, as in previous cases. In the crystal structure of Mg-bearing rhodonite, most of the Mg is concentrated at the smallest *M*4 polyhedron, with the average *M*–O distance of 2.1 Å (Peacor et al. 1978). In Zn-bearing rhodonite Mn, Zn and Ca are statistically distributed among four sites *M*1, *M*2, *M*3, and *M*4, but most of the Zn is concentrated at *M*4 (Nelson and Griffen 2005). The main feature of so-called «Ca–Mg–Fe-rhodonite» is the common occurrence of Mn, Mg, Fe at *M*1, *M*2, *M*3, *M*4 sites whereas the *M*5 site is predominantly occupied by Ca (Leverett et al. 2008).

Table 3 Crystal parameters, data collection, and structure refinement details for ferrorhodonite

Crystal data	
Formula	$CaMn_3FeSi_5O_{15}$
Formula weight (g)	644.1
Temperature (K)	293
Crystal system	Triclinic
Space group	$P\bar{1}$
a (Å)	6.6766 (5)
b (Å)	7.6754 (6)
c (Å)	11.8032 (9)
α (°)	105.500 (1)
β (°)	92.275 (1)
γ (°)	93.918 (1)
V (Å^3)	580.44 (1)
Z	1
Calculated density, D_x (g cm^{-3})	3.69
Crystal size (mm)	0.10 × 0.12 × 0.13
Crystal form	Anhedral grain
Data collection	
Diffractometer	SMART APEX2 CCD
Radiation; λ	MoK_α; 0.71073
Absorption coefficient, μ (mm^{-1})	2.795
F (000)	624
Data range θ (°); h, k, l	1.79–30.80; $-9 < h < 9$, $-10 < k < 11$, $-16 < l < 16$
No. of measured reflections	7879
Total reflections (N_2)/unique(N_1)	3605/3114
Criterion for observed reflections	$I > 2\sigma(I)$
R_{int} (%)	3.14
$R\sigma$ (%)	4.03
Refinement	
Refinement on	Full-matrix least squares on F
Weight scheme	$1/(\sigma^2\lvert F\rvert + 0.002025\ F^2)$
R_1 (%), wR_2 (%)	4.02, 6.30
GOF (Goodness of fit)	0.99
Max./min. residual e density, (eÅ^{-3})*	0.84/−1.56

* The position of $\Delta\rho_{max}$ is in the space between $M1$, $M2$, and $M5$ sites; the position of $\Delta\rho_{min}$ is at the $M2$ site

Table 4 Fractional coordinates, site occupancies, and equivalent displacement parameters of atoms (U_{eq}, Å^2) in the structure of ferrorhodonite

Site	x	y	z	U_{eq}	Composition
$M1$	0.9685 (1)	0.8821 (1)	0.8524 (1)	0.0054 (2)	Mn
$M2$	0.8755 (1)	0.6829 (1)	0.5556 (1)	0.0055 (2)	Mn
$M3$	0.8127 (1)	0.4920 (1)	0.2706 (1)	0.0061 (2)	Mn
$M4$	0.8002 (1)	0.3031 (1)	0.9768 (1)	0.0119 (2)	Fe
$M5$	0.6398 (2)	0.0456 (1)	0.6942 (1)	0.0102 (2)	$Ca_{0.81}Mn_{0.19}$
$T1$	0.4967 (1)	0.2196 (1)	0.1247 (1)	0.0047 (3)	Si
$T2$	0.6370 (2)	0.2682 (1)	0.4708 (1)	0.0044 (3)	Si
$T3$	0.7079 (2)	0.4607 (1)	0.7390 (1)	0.0044 (3)	Si
$T4$	0.7533 (2)	0.7449 (1)	0.0897 (1)	0.0044 (3)	Si
$T5$	0.8448 (2)	0.9259 (1)	0.3466 (1)	0.0039 (2)	Si
O1	0.9630 (4)	0.9534 (3)	0.6774 (2)	0.0081 (7)	O
O2	0.8946 (4)	0.6003 (3)	0.7318 (2)	0.0083 (7)	O
O3	0.8887 (4)	0.7512 (3)	0.3899 (2)	0.0081 (7)	O
O4	0.8090 (4)	0.3993 (3)	0.4363 (2)	0.0081 (7)	O
O5	0.8068 (4)	0.5505 (3)	0.0996 (2)	0.0104 (8)	O
O6	0.7357 (4)	0.1998 (3)	0.1304 (2)	0.0079 (7)	O
O7	0.7460 (4)	0.3254 (3)	0.8172 (2)	0.0111 (8)	O
O8	0.6601 (4)	0.9313 (3)	0.8530 (2)	0.0071 (7)	O
O9	0.4467 (4)	0.2577 (3)	0.9955 (2)	0.0081 (7)	O
O10	0.5832 (4)	0.7449 (4)	0.5881 (2)	0.0119 (8)	O
O11	0.9419 (4)	0.8438 (3)	0.0414 (2)	0.0074 (7)	O
O12	0.5147 (4)	0.5802 (3)	0.7791 (2)	0.0074 (7)	O
O13	0.6283 (4)	0.3173 (3)	0.6142 (2)	0.0080 (7)	O
O14	0.6997 (4)	0.0551 (3)	0.4364 (2)	0.0093 (7)	O
O15	0.6986 (4)	0.8616 (3)	0.2228 (2)	0.0063 (7)	O

Cation arrangement in our ferrorhodonite from Broken Hill is expected to be relatively unusual because of a high content of Fe^{2+}. The interpretation of the structural refinement data leads to the following conclusions: the $M1$, $M2$, and $M3$ sites are octahedrally coordinated, with average M–O distances of 2.214, 2.209, and 2.222 Å, respectively, which is appropriate for Mn or a statistical occupancy of Mn and Fe with Mn predominance. The $M4$-centered polyhedron (see Figs. 5, 6) can be considered as five-coordinated with the shortest M–O distance 1.96 Å, as noted by Peacor and Niizeki (1963), or, including the longest $M4$-O8 bond (2.8 Å), this site could be considered as a distorted six-coordinated polyhedron, especially, when in this site there is sufficient amount of Mn (Fig. 6). In our case, the shortest interatomic distance 1.9 Å at the $M4$ site is not quite suitable for high content of Mn, with ionic radius 0.83 Å (Shannon and Prewitt 1969); thus, we assume this polyhedron to be predominantly occupied by a cation of smaller ionic radius. The most irregular seven-coordinated polyhedron $M5$ is occupied by 0.8 Ca and 0.2 Mn, which is verified by the number of electrons ($e_{ref} = 21$).

Mössbauer spectroscopy data and final formula of ferrorhodonite

The most difficult point of our research was connected with the obtaining of convincing evidences of Fe arrangement between the M sites. Previous researchers who

Table 5 Anisotropic atomic displacement parameters for ferrorhodonite

Site	U_{11}	U_{22}	U_{33}	U_{12}	U_{13}	U_{23}
*M*1	0.0044 (3)	0.0052 (2)	0.0067 (3)	0.0013 (2)	−0.0002 (2)	0.0012 (2)
*M*2	0.0050 (3)	0.0065 (2)	0.0050 (2)	0.0006 (2)	0.0001 (2)	0.0012 (2)
*M*3	0.0055 (3)	0.0061 (2)	0.0067 (3)	0.0007 (2)	−0.0006 (2)	0.0014 (2)
*M*4	0.0142 (3)	0.0153 (3)	0.0082 (2)	0.0072 (2)	0.0028 (2)	0.0047 (2)
*M*5	0.0085 (3)	0.0054 (3)	0.0153 (3)	0.0000 (2)	0.0014 (3)	0.0004 (2)
*T*1	0.0031 (4)	0.0059 (4)	0.0050 (4)	0.0005 (3)	−0.0002 (3)	0.0011 (3)
*T*2	0.0040 (4)	0.0057 (4)	0.0036 (4)	0.0005 (3)	0.0004 (3)	0.0015 (3)
*T*3	0.0037 (4)	0.0057 (4)	0.0040 (4)	0.0004 (3)	0.0009 (3)	0.0013 (3)
*T*4	0.0040 (4)	0.0058 (4)	0.0036 (4)	0.0001 (3)	0.0002 (3)	0.0019 (3)
*T*5	0.0037 (4)	0.0033 (4)	0.0046 (4)	0.0003 (3)	0.0005 (3)	0.0010 (3)
O1	0.006 (1)	0.007 (1)	0.008 (1)	−0.001 (1)	0.001 (1)	0.001 (1)
O2	0.005 (1)	0.008 (1)	0.010 (1)	0.000 (1)	0.001 (1)	0.002 (1)
O3	0.012 (1)	0.005 (1)	0.006 (1)	0.001 (1)	−0.002 (1)	0.002 (1)
O4	0.008 (1)	0.007 (1)	0.009 (1)	0.001 (1)	0.001 (1)	0.004 (1)
O5	0.014 (14)	0.009 (1)	0.009 (1)	0.002 (1)	−0.001 (1)	0.004 (1)
O6	0.005 (1)	0.011 (1)	0.008 (1)	0.002 (1)	−0.000 (1)	0.004 (1)
O7	0.014 (1)	0.011 (1)	0.009 (1)	0.001 (1)	−0.002 (1)	0.005 (1)
O8	0.007 (1)	0.006 (1)	0.008 (1)	0.000 (1)	0.001 (1)	0.003 (1)
O9	0.008 (1)	0.011 (1)	0.004 (1)	−0.000 (1)	−0.001 (1)	0.003 (1)
O10	0.004 (1)	0.020 (1)	0.012 (1)	−0.002 (1)	−0.002 (1)	0.008 (1)
O11	0.007 (1)	0.007 (1)	0.008 (1)	−0.000 (1)	0.001 (1)	0.003 (1)
O12	0.006 (1)	0.006 (1)	0.006 (1)	0.001 (1)	0.000 (1)	−0.003 (1)
O13	0.010 (1)	0.009 (1)	0.003 (1)	−0.001 (1)	−0.000 (1)	0.001 (1)
O14	0.010 (1)	0.007 (1)	0.009 (1)	0.001 (1)	0.005 (1)	−0.001 (1)
O15	0.005 (1)	0.010 (1)	0.003 (1)	0.001 (1)	−0.001 (1)	0.002 (1)

investigated rhodonite by Mössbauer spectroscopy concluded that Fe^{2+} could be distributed among the five possible cation sites: most of iron is in *M*1, *M*2, and *M*3 (Dickson 1975). In our case, the large difference in IS and QS values of doublets in the rhodonite Mössbauer spectrum strongly suggests that Fe^{2+} occupies more than one distinct crystallographic site in the structure. The doublet with high QS that dominates at the spectrum of ferrorhodonite likely corresponds to one or more distorted octahedral sites in the structure (*M*4, *M*5), whereas the less intense doublet with lower QS corresponds to one of the less distorted sites (*M*1, *M*2, *M*3). However, we decided to exclude possibility of occupancy of the *M*5 site by Fe because of very long bond distances, 2.565 and 2.512 Å, which are not appropriate for Fe^{2+}, with ionic radius 0.78 Å (Shannon and Prewitt 1969). It seems reasonable to assume that 62.5 ± 2% Fe occupies the distorted *M*4 polyhedron, whereas 37.5 ± 2% Fe is distributed between less distorted octahedra *M*1, *M*2, and *M*3. The Mössbauer data on Fe distribution among the *M* sites in rhodonite reported by Dickson (1975) and Griffen and Nelson (2007) demonstrate that doublet with small quadrupole splitting and low IS was assigned to Fe^{2+} cation at the *M*4 site, which has sixfold coordination with one short *M*–O bond. This doublet has a smaller relative area than doublets corresponding to Fe^{2+} at the *M*1, *M*2, and *M*3 sites. Therefore, the authors concluded that most of the iron is in the octahedrally coordinated *M*1, *M*2, and *M*3 sites, though the iron shows some preferences for the *M*4 site.

In Table 8 we present two different approaches for interpretation our Mössbauer data: the conventional method, used by Dickson (1975) and Griffen and Nelson (2007), and our suggestion. In this work, we based on the interpretation theoretically and empirically verified by patterns described by Dyar et al. (2006). The correlation between spin state of Fe ions, the number of coordinating atoms, type of anion, distortion of local environment and values of central or isomer shift, and quadrupole splitting have been used in our interpretation of the Mössbauer spectrum of ferrorhodonite. The basic rules of thumb are the following:

Table 6 Interatomic distances for cation sites and distortion parameters for *M*1–*M*5 sites in the crystal structure of ferrorhodonite

*M*1	O8	2.119 (1)	*T*1	O8	1.589 (1)
	O6	2.130 (1)		O6	1.613 (1)
	O11	2.170 (1)		O9	1.654 (1)
	O2	2.258 (1)		O12	1.656 (1)
	O1	2.273 (1)			<1.628>
	O11	2.337 (1)	*T*2	O10	1.586 (1)
		<2.215>		O4	1.610 (1)
$\Delta^{M(1)}$		13.097		O13	1.636 (1)
*M*2	O10	2.067 (1)		O14	1.664 (1)
	O3	2.159 (1)			<1.624>
	O1	2.211 (1)	*T*3	O7	1.589 (1)
	O4	2.245 (2)		O2	1.607 (1)
	O4	2.258 (1)		O13	1.630 (1)
	O2	2.331 (1)		O12	1.644 (1)
		<2.212>			<1.618>
$\Delta^{M(2)}$		14.032	*T*4	O5	1.590 (1)
*M*3	O2	2.121 (1)		O11	1.626 (1)
	O3	2.122 (1)		O9	1.635 (1)
	O5	2.181 (1)		O15	1.655 (1)
	O12	2.234 (2)			<1.627>
	O4	2.252 (1)	*T*5	O3	1.597 (1)
	O6	2.413 (1)		O1	1.610 (1)
		<2.221>		O14	1.641 (1)
$\Delta^{M(3)}$		20.058		O15	1.664 (1)
*M*4	O7	1.958 (1)			<1.628>
	O5	2.053 (1)			
	O11	2.109 (1)			
	O6	2.210 (1)			
	O9	2.390 (1)			
	O8	2.908 (1)			
		^{5} < 2.144>			
		^{6} < 2.271>			
$^{5}\Delta^{M(4)}$		47.843			
$^{6}\Delta^{M(4)}$		191.167			
*M*5	O8	2.274 (2)			
	O7	2.294 (1)			
	O10	2.310 (1)			
	O1	2.315 (1)			
	O13	2.512 (1)			
	O15	2.565 (1)			
	O14	2.638 (1)			
		<2.415>			
$\Delta^{M(5)}$		33.602			

Polyhedral distortion (Δ) is defined as $\Delta = (1/n)\sum_{i=1-n}\{[(M\text{–O})_i - \langle M\text{–O}\rangle]/\langle M\text{–O}\rangle\}^2 \times 10^4$ (Brown and Shannon 1973)

Table 7 Cation arrangement in structurally studied samples of rhodonite and ferrorhodonite

Mineral	Octahedral sites					References
	*M*1	*M*2	*M*3	*M*4	*M*5	
Rhodonite	Mn	Mn	Mn	Mn, Mg, Fe	Ca, Mn	Peacor and Niizeki (1963)
Mg-bearing rhodonite	$Mn_{0.89}Mg_{0.11}$	$Mn_{0.86}Mg_{0.14}$	$Mn_{0.86}Mg_{0.14}$	$Mn_{0.53}Mg_{0.47}$	$Ca_{0.60}Mn_{0.40}$	Peacor et al. (1978)
Rhodonite	Mn, Mg	Mn, Mg	Mn, Mg	Mn, Fe, Mg	Mn, Ca	Ohashi and Finger (1975)
Rhodonite	Mn, Fe	Mn, Fe	Mn, Ca	Mn, Mg, Fe, Zn	Mn, Ca	Nelson and Griffen (2005)
Zn-rhodonite	Mn, Fe, Ca	Mn, Ca, Fe	Mn, Ca, Fe	Mn, Zn, Fe, Mg	Ca, Mn, Fe	Nelson and Griffen (2005)
«Ca,Mg,Fe-rhodonite»	Mn, Mg, Fe	Mn, Mg, Fe	Mn, Mg, Fe	Mn, Mg, Fe	Ca, Mn, Fe	Leverett et al. (2008)
Ferrorhodonite	Mn, Fe	Mn, Fe	Mn, Fe	$Fe_{0.81}$ $Mn_{0.12}Mg_{0.04}Zn_{0.03}$	$Ca_{0.81}Mn_{0.19}$	Present paper

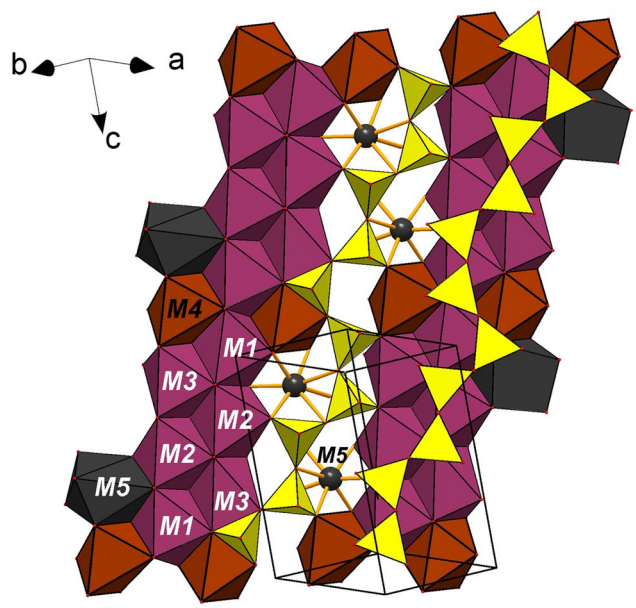

Fig. 4 General view of the crystal structure of ferrorhodonite

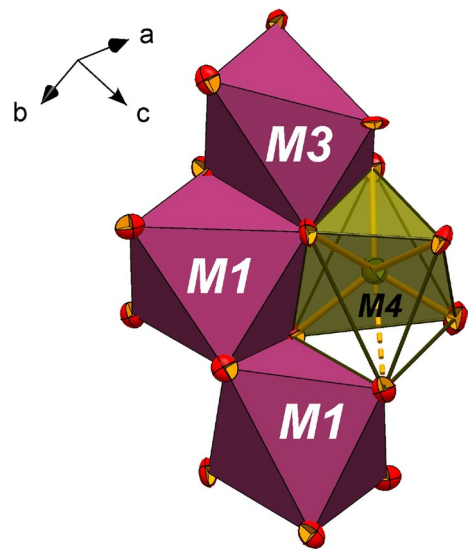

Fig. 5 Arrangement and surroundings of the distorted *M*4 polyhedron in the structure of ferrorhodonite

the larger the QS, the more distorted the coordination polyhedron surrounding the Fe atom; the smaller the IS, the more covalent bonds between anions and cations; the larger the IS, the larger the number of coordinating atoms around Fe. Based on these rules we conclude that the doublet with high QS of 2.4 mm s^{-1} and IS = 1.19 mm s^{-1} and relative area 62.5 ± 2% corresponds to Fe^{2+} at the most distorted site *M*4 with distortion value ($^{[5]}\Delta^{M(4)}$ = 47.843; $^{[6]}\Delta^{M(4)}$ = 191.166) and irregular six-coordination with the shortest *M*–O distance, 1.958 Å. The doublet with the lower QS of 1.3 mm s^{-1} IS of 1.06 mm s^{-1} and relative area of 37.5 ± 2% can be assigned to the *M*1, *M*2, and *M*3 sites, less distorted and characterized by shorter average interatomic *M*–O distances. Taking into account these considerations, the crystal-chemical formula of ferrorhodonite can be written as follows ($Z = 2$):

$^{M5}(Ca_{0.81}Mn_{0.19})\,^{M1-3}(Mn_{2.52}Fe_{0.48})\,^{M4}(Fe^{2+}_{0.81}Mn_{0.12}Mg_{0.04}Zn_{0.03})\,[Si_5O_{15}]$.

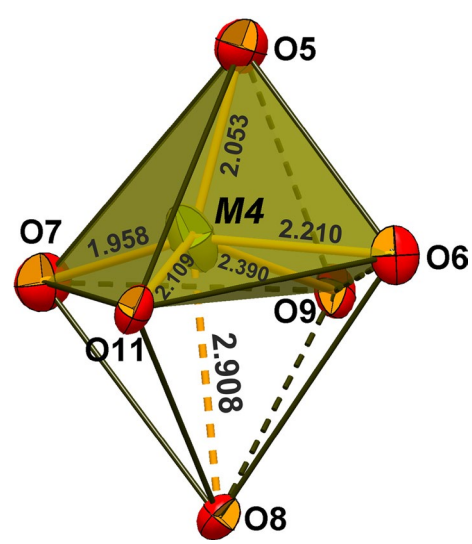

Fig. 6 Arrangement of O atoms around the *M*4 site in the structure of ferrorhodonite

Table 8 Parameters of Mössbauer doublet for ferrorhodonite and the occupancies of *M*1–*M*4 sites according to the two different methods

Mössbauer doublet		
Doublet	Light gray	Dark gray
IS (mm s^{-1})	1.06	1.19
QS (mm s^{-1})	1.29	2.42
Area ratio (%)	37.5	62.50
Fe (*apfu*)	0.48	0.79
Oxidation state of Fe	Fe^{2+}	Fe^{2+}
Case (1)	Conventional	
Assignment	Fe^{2+} at *M*4	Fe^{2+} at *M*1–*M*3
Case (2)	Our suggestion	
Assignment	Fe^{2+} at *M*1–*M*3	Fe^{2+} at *M*4

	Case (1) conventional method	Case (2) our suggestion
*M*1–*M*3	$Mn_{2.21}Fe^{2+}{}_{0.79}$	$Mn_{2.52}Fe^{2+}{}_{0.48}$
*M*4	$\mathbf{Fe^{2+}_{0.48}}Mg_{0.04}Zn_{0.03}Mn_{0.45}$	$\mathbf{Fe_{0.79}{}^{2+}}Mg_{0.04}Zn_{0.03}Mn_{0.14}$
*M*5	$Ca_{0.79}Mn_{0.21}$	$Ca_{0.79}Mn_{0.21}$

However, in both cases (conventional and our) Fe^{2+} is the dominant cation at *M*4 site, and, consequently, the simplified formula can be represented as ${}^{M5}Ca^{M1-M3}Mn_3^{M4}Fe^{2+}[Si_5O_{15}]$.

Acknowledgements We are grateful to Robert F. Martin and anonymous reviewer for valuable comments. This study was supported by the Russian Science Foundation, Grant No. 14-17-00048 (in part of mineralogical studies) and Foundation of the President of the Russian Federation, Grant No. MK-8033.2016.5 (refinement of the crystal structure). The electron-microprobe analyses were performed at the Laboratory of Analytical Techniques of High Spatial Resolution, Department of Petrology, Moscow State University, using a microprobe instrument JEOL JXA-8230 purchased with the financial support by the Program for Development of MSU.

References

Back ME (2014) Fleischer's glossary of mineral species. The Mineral Rec Inc, Tucson

Birch WD (1999) Minerals of Broken Hill. Broken Hill City Council, Australia

Brandenburg K, Putz H (2005) DIAMOND version 3. Crystal Impact GbR, Bonn

Brown ID, Shannon RD (1973) Empirical bond strength–bond length curves for oxides. Acta Crystallogr A 29:266–282

Bruker (2009) APEX2 and SAINT. Bruker AXS Inc, Madison

Chukanov NV (2014) Infrared spectra of mineral species: extended library. Springer, Dordrecht

Dickson BL (1975) The iron distribution in rhodonite. Am Mineral 60:98–104

Dyar MD, Agresti DG, Schaefer MW, Grant CA, Sklute EC (2006) Mössbauer spectroscopy of earth and planetary materials. Annu Rev Earth Planet Sci 34:83–125

Frost RB, Mavrogenes JA, Tomkins AG (2002) Partial melting of sulfide ore deposits during medium- and high-grade metamorphism. Can Mineral 40:1–18

Frost RB, Swapp SM, Gregory RW (2005) Prolongedd existence of sulfide melt in the Broken Hill orebody, New South Wales, Australia. Can Mineral 43:479–493

Griffen DT, Nelson WR (2007) Mössbauer spectroscopy of Zn-poor and Zn-rich rhodonite. Am Mineral 92:1486–1491

Henderson EP, Glass JJ (1936) Pyroxmangite, a new locality: identity of sobralite and pyroxmangite. Am Mineral 21:273–294

Hietanen A (1938) On the petrology of Finnish quartzites. Bull Comm Geol Finl 122:1–119

Ibers JA, Hamilton WC (eds) (1974) International tables for X-ray crystallography, vol IV. The Kynoch Press, Birmingham

Leverett P, Williams PA, Hibbs DE (2008) Ca-Mg-Fe-rich rhodonite from the Morro da Mina mine, Conselheiro Lafaiete, Minas Gerais, Brasil. Mineral Rec 44:149–184

Liebau F, Hilmer W, Lindemann G (1959) Über die Kristallstruktur des Rhodonit (Mn, Ca)SiO3. Acta Crystallogr 12:182–187

Mason B (1973) Manganese silicate minerals from Broken Hill, New South Wales. J Geol Soc Aust 20:397–404

Nelson WR, Griffen DT (2005) Crystal chemistry of Zn-rich rhodonite ("fowlerite"). Am Mineral 90:969–983

Ohashi Y, Finger LW (1975) Pyroxenoids: a comparison of refined structures of rhodonite and pyroxmangite. Carnegie Inst Wash Year Book 74:564–569

Peacor DR, Niizeki N (1963) The redetermination and refinement of the crystal structure of rhodonite. (Mn, Ca)SiO_3. Z Kristallogr 119:98–116

Peacor DR, Essene EJ, Brown PE, Winter GA (1978) The crystal chemistry and petrogenesis of a magnesian rhodonite. Am Mineral 63:1137–1142

Petříček V, Dušek M, Palatinus L (2006) Jana 2006. Structure determination software programs. Institute of Physics, Praha

Prescher C, McCammon C, Dubrovinsky L (2012) MossA—a program for analyzing energy-domain Mössbauer spectra from conventional and synchrotrone sources. J Appl Crystallogr 45:329–331

Minerals. Reference book (1981) vol 3, part. 2, Nedra Publishing, Moscow **(in Russian)**

Shannon RD, Prewitt CT (1969) Effective ionic radii in oxides and fluorides. Acta Crystallogr. B 25:925–946

Walters SG (1998) Broken Hill-type deposits. J Aust Geol Geophys 17(4):229–237